European Conference on Computational Fluid Dynamics
ECCOMAS CFD 2006
P. Wesseling, E. Oñate and J. Périaux (Eds)

A JOINT DATA ASSIMILATION - COUPLING ALGORITHM APPLIED TO SHALLOW WATER FLOOD MODELS

I.Yu. Gejadze* **and J. Monnier†**

LMC-IMAG, INRIA Rhône-Alpes, MOISE project
BP 53, 38041 Grenoble Cedex 9, France
* e-mail: igor.gejadze@imag.fr
† e-mail: jerome.monnier@imag.fr
web page: www-lmc.imag.fr/lmc-edp/Jerome.Monnier

Key words: Weak coupling, Superposed 'zoom' model, Shallow-water, Optimal control, Data assimilation, Flood modeling

Abstract. *In the context of river hydraulics, we develop the idea of a richer local zoom model superposed to a given global model. The local zoom model (2D shallow water equations in flooded parts) describes additional physical phenomena which are not represented by the basic global model (1D shallow-water equations with storage area). The weak coupling method presented preserves the integrity of the global 1D model, while it allows to calibrate its input variables (inflow boundary conditions for example) by assimilating local data measured inside the 2D zoom area. The resulting Joint Assimilation Coupling algorithm (JAC) is based on the optimal control method of PDEs systems. Some numerical tests, where we consider a toy flooding event that involves overflowing of the main channel and a moving front travelling over previously dry areas, show the efficiency of the algorithm.*

1 INTRODUCTION

Generally, operational hydrological models describing river networks are based on the 1D shallow water equations with storage areas, essentially because of their low computational cost required for fast decision-making. The bi-dimensional situations, such as those that occur during flooding, are represented by the storage areas i.e. by extra source terms in the 1D equations. In the present study, we seek to model the 2D flows in the local flooded areas, coupled in a certain way with the 1D-net global model. Another reason for using local 2D models arises in the context of Data Assimilation (DA): this can allow to assimilate data which are not described in the 1D model.
A natural way to introduce local 2D models could be the Domain Decomposition Method (DDM), when one obtains a set of 1D channels and 2D areas/junctions, see e.g. [1],[2]. The coupling techniques which can be applied in this case vary from the classical Schwarz

method with overlapping, the wave-form relaxation method , see e.g. [3], (which is a subset of the global time Schwartz method), to the optimal control based methods, [4]. When the DDM is applied, the integrity of the existing 1D-net model is not preserved and a new composite model has to be created. Indeed, the DDM disintegrates the model making available a parallel implementation. Here, we keep in mind a different approach, proceeding from the condition that the 1D-net global model must stay intact. This may be considered as a natural demand from the expert-users that holds this model in operational use.

Thus, we suggest a coupling principle, which may be called superposed rather than decomposed: we keep the overall integrity of the existing 1D model. Source terms of the 1D model within the areas of interest (storage areas) are estimated via the 2D local solution as a defect correction, [5]. The 1D model, in turn, provides a key part of Boundary Conditions (BC) at open boundaries of the 2D local 'zoom' superposed model. BCs and all information transfers between both models are based on the incoming characteristics, which can be viewed as a special case of absorbing BC, [6], [7].

Thus, the 2D local model is 'superposed' over the 1D model in the 'storage areas' and plays the role of a zoom. Both producing the 2D estimation of the flow and improving performance of the 1D global model.

Let us point out that the two models are not consistent since: a) the 1D model cannot provide the full set of BC for the 2D model; b) the 1D model is usually solved on much coarser mesh with a typical ratio $10^1 - 10^2$ for the space mesh size and $10^2 - 10^3$ for the time step. We compensate the lack of information by using a-priori information measured data (variationnal data assimilation), and the difference of the spatio-temporal grids is circumvented by using weak coupling terms (mortar type approach).

Eventually, we obtained what we call the Joint Assimilation Coupling (JAC) algorithm, which solves simultaneously both DA and superposed weak coupling. It is based on the optimal control method of PDEs systems. We specify an extended objective functional such that in addition to the usual DA terms (residuals between model predictions and measured data), it includes coupling conditions written in an integral form.

The main advantages of this algorithm are the following: 1) no additional assumptions are needed since it evades difficulties of coupling inconsistent models; 2) one can assimilate data within the 'zoom' area which are not represented into the 1D model, allowing to identify its parameters or input variables (inflow BC for example).

The extended objective functional is minimized using the quasi-Newton LBFGS algorithm, while the gradient is computed using the adjoint method. We conduct numerical tests, where we consider a toy flooding event that involves overflowing of the main channel and a moving front travelling over previously dry areas.

2 MATHEMATICAL MODEL

2.1 2D model

The 2D problem is considered in the domain Ω_2 ('zoom' area) confined by the boundaries $\Gamma_{3,4,5,6}$ and the main channel (domain Ω_1) is confined by the boundaries $\Gamma_{1,2}$, see Fig.1. For simplicity we assume that the positions of the lateral boundaries $\Gamma_3(t)$ and $\Gamma_4(t)$ (inflow and outflow respectively) are fixed along the median curve of the main channel (x' axis), but they can stretch in the tangential direction y' as long as the 'zoom' area evolves in time. The boundaries $\Gamma_5(t)$, $\Gamma_6(t)$ represent moving wet/dry fronts. The bathymetry is given by the function $Z(x, y)$.

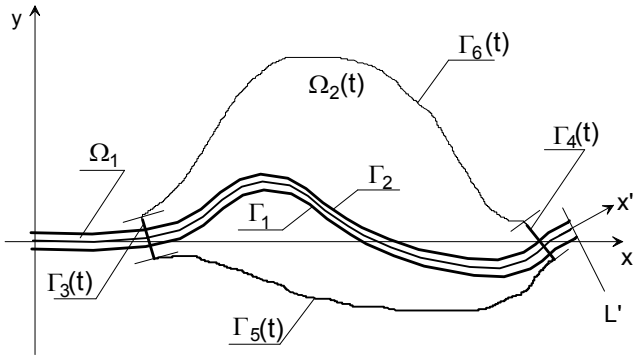

Figure 1: General problem layout.

The equations describing the 2D shallow water flow are as follows:

$$U_t + A(U)_x + B(U)_y - S(U) = 0, \quad (x, y) \in \Omega_2(t), \quad t \in (0, T) \tag{1}$$

with $U = [\ h,\ q,\ p\ ]^T$, $A(U) = [\ q,\ q^2/h + gh^2/2,\ qp/h\ ]^T$, $B(U) = [\ p,\ pq/h,\ p^2/h + gh^2/2\ ]^T$ and $S(U) = [\ 0,\ gh(Z_x - f_x),\ gh(Z_y - f_y)\ ]^T$.

Here $h = h(x, y, t)$ is the surface elevation, $q = q(x, y, t)$ and $p = p(x, y, t)$ are components of discharge, Z_x, f_x and Z_y, f_y are the bed slope and the friction slope associated to the x and y axes respectively, g is the gravity acceleration. The friction slope is defined using the Manning law via the Manning coefficient $\mu = \mu(x, y)$ as follows:

$$f_x = \mu^2(q^2 + p^2)^{1/2} q h^{-10/3}; \quad f_y = \mu^2(q^2 + p^2)^{1/2} p h^{-10/3}$$

We consider the 2D local SWE model with open lateral boundaries using the first order absorbing BC that is essentially the incoming characteristics, see [6], [7]. Assuming that the flow at $\Gamma_{3,4}$ always remains subcritical, we set:

$$(x, y) \in \Gamma_3 : \quad q_{\vec{n}} + ch = w_1(x, y, t), \quad q_{\vec{\tau}} = w_3(x, y, t), \ \forall u_{\vec{n}} > 0 \tag{2}$$

$$(x,y)\in\Gamma_4:\ \ q_{\vec{n}}-ch=w_2(x,y,t),\ \ q_{\vec{\tau}}=w_3(x,y,t),\ \forall u_{\vec{n}}<0 \tag{3}$$

where $q_{\vec{n}}$ and $q_{\vec{\tau}}$ are the normal and tangent (with respect to the boundary) components of the discharge, $c=(gh)^{1/2}$ is the celerity. The quantities $w_k(x,y,t)$ are imposed. In all the sequel, initial condition is given.

2.2 1D model with storage area

The 1D model can be derived from the 2D SWE model in two steps.
First, the 2D model has to be considered in the 'channel-following' coordinate system (x',y'), when x'-axis follows the median curve of the main channel and y' is the orthonormal to x'. Assuming that the median curve is given in the parametric form $x_m=m_1(x'),\ y_m=m_2(x')$ we can obtain the following co-ordinate transformation

$$\frac{\partial x'}{\partial x}=\frac{cos(\alpha')}{1-y'\alpha'_x},\ \ \frac{\partial y'}{\partial x}=-sin(\alpha'),\ \ \frac{\partial x'}{\partial y}=\frac{sin(\alpha')}{1-y'\alpha'_x},\ \ \frac{\partial y'}{\partial x}=cos(\alpha')$$

where α' is the angle between the x-axis and the local tangent to the median curve, $\alpha'_x=\partial\alpha'/\partial x$. By neglecting $y'\alpha'_x$ (that is often justified for river flows), we obtain the same equations as (1) for the variables $U'=[\ h,q',p'\ ]^T$, where q',p' are the normal and tangent component of discharge in the new co-ordinate system (x',y').
The second step is to integrate these equations in y' from Γ_1 to Γ_2. Assuming that: a) zero fluxes through $\Gamma_{1,2}$; b) $u'_{y'}=0$; c) $(h_{x'})_{y'}=0$ we get the Saint-Venant equations or, in the case when the main channel has a constant rectangular cross-section of width b, the 'dimensional' 1D SWE as follows

$$\tilde{U}'_t+\tilde{A}(\tilde{U}')_{x'}-\tilde{S}(\tilde{U}')=\Psi,\ \ (x')\in(0,L'),\ \ t\in(0,T) \tag{4}$$

with: $\tilde{U}'=[\ H',\ Q'\ ]^T$, $\tilde{A}(\tilde{U}')=[\ Q',\ (Q')^2/H'+g(H')^2/2\ ]^T$, $\tilde{S}(\tilde{U}')=[\ 0,\ gh(Z'_x-f'_x)\ ]^T$ and $\Psi=[\psi_1,\ \psi_2]^T$. Where H' is the wet cross-section area and Q' is the total discharge. If H' and Q' are scaled by b, we get the classical 1D SWE variables.

Above, we have artificially introduced the source terms $\Psi=[\psi_1,\ \psi_2]^T$ to actuate the 1D solution. We assume that these are existing entries into the standard 1D model with storage areas (since storage areas are represented by source terms anyway).

Similarly to the 2D case, we consider first order absorbing BC, based on incoming characteristics. We impose:

$$x'=0:\ Q'+c'H'=W_1(0,t) \tag{5}$$

$$x'=L':\ Q'-c'H'=W_2(L',t) \tag{6}$$

where $c' = (gH'/b)^{1/2}$. The initial condition is given.

It is worth mentioning that the characteristic BC for the 1D model is not an obligatory option. We use it for convenience, but one could use the classical BC $Q'(0,t),\ H'(L',t)$. These are, however, reflective BC.

3 FINITE VOLUME SCHEMES

The SWE are solved numerically in the conservative form by the finite-volume method. For simplicity we utilize a structured rectangular mesh, although the solver allows non-structured mesh computations.

3.1 2D scheme

We reduce the 2D SWE problem to a set of 1D local Riemann problems, from where integral fluxes between adjacent cells can be retrieved, Fig.2. Let us consider a mesh consisting of finite volumes K_i covering the 'zoom' area (Ω_2) in such a way that volume interfaces continuously reproduce boundaries of the main channel ($\Gamma_{1,2}$) as shown in Fig.2. In general case the mesh not necessarily must be quadrangular.

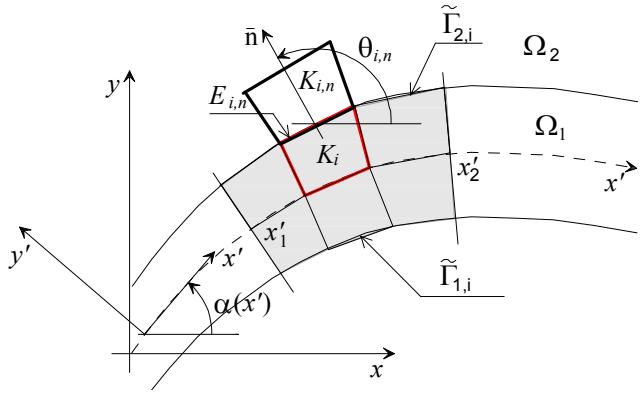

Figure 2: Finite volume mesh

Assuming the Euler explicit time discretization, for the finite volume K_i the model equations (1) are approximated as follows

$$U_i(t_m+\tau) = U_i(t_m) - \tau \left(\frac{1}{|K_i|} \sum_{n=1}^{4} F_n(U_i) - S(U_i) \right)_{t=t_m} \tag{7}$$

where $m = 0, ..., T/\tau$ is the time index, τ is the time step used for the 2D model integration, $F_n(U_i)$ are total fluxes of U via n^{th} edge $E_{i,n}$ of the volume K_i and $|K_i|$ is the

volume surface. For the edge we define a rotation

$$T(\theta) = \begin{pmatrix} 1 & 0 & 0 \\ 0 & cos(\theta) & sin(\theta) \\ 0 & -sin(\theta) & cos(\theta) \end{pmatrix}$$

where θ is the angle between the normal $\vec{n}$ to the edge $E_{i,n}$ and the x-axis. Variables $V = [\ h,\ q_{\vec{n}},\ q_{\vec{\tau}}]$ are used to define a vector of local Godunov fluxes as follows

$$\Phi(V) = \left[q_{\vec{n}},\ q_{\vec{n}}^2/h + gh^2/2,\ q_{\vec{n}}q_{\vec{\tau}}/h\right]^T$$

Computing the flux $F_n(U_i)$ consists of three steps, see e.g. [8].
First we compute the normal and tangent discharge components in two finite volumes K_i and $K_{i,n}$ adjacent to the edge $E_{i,n}$ (see Fig.2) using the rotation as follows $V_i = T(\theta_{i,n})U_i$.
Second, we compute $\Phi(V)$ as an approximate solution of the local Riemann problem

$$\frac{\partial V}{\partial t} = \frac{\partial \Phi(V)}{\partial x_{\vec{n}}}, \quad V(x,0) = \left\{ \begin{array}{ll} V_i, & x_{\vec{n}} < 0 \\ V_{i,n}, & x_{\vec{n}} > 0 \end{array} \right\}$$

To this end, we use an approximate HLLC solver described in details in [8]. This first order scheme handles correctly the transition between sub-critical and super-critical flows, unlike most other first order schemes, that is important for a reliable front propagation modeling.
The last step is to compute fluxes of U_i using the inverse rotation $T^{-1}(\theta_{i,n})$, so we can eventually write

$$F_n(U_i) = T^{-1}(\theta_{i,n})\Phi(V) \tag{8}$$

The bed slope is included into the source term of the 1D local Riemann problem in the manner as described in [9], thus we deal with the non-homogeneous version of the HLLC scheme. We use a simple treatment of a dry/wet front introducing a front propagation threshold. If the surface elevation is less than the threshold value, then zero fluxes between sells are specified.

For those control volumes belonging to Ω_1 the variables in the channel-following coordinates U', as well as fluxes $F_n(U_i')$ can be obtained using another rotation $T(\alpha')$ (see Fig.(2) for the definition of α) as follows

$$U' = T(\alpha')U, \quad F_n(U') = T(\alpha')F_n(U)$$

The numerical implementation of the characteristic BC is as follows. Let us consider the 'inlet' boundary Γ_3, for example. We compute the elevation and the discharge components in 'ghost' cells $K_{i,n},\ \forall E_{i,n} \in \Gamma_3$, adjacent and symmetric to the boundary sells K_i as follows

$$h(t)|_{(x,y)\in K_i} = Z + \frac{1}{2}\left(\frac{w_1}{c} - \frac{w_2}{c}\right)$$

$$q_{\vec{n}}(t)|_{(x,y)\in K_i} = \frac{1}{2}\left[\left(1+\frac{u_{\vec{n}}}{c}\right)w_1 + \left(1-\frac{u_{\vec{n}}}{c}\right)w_2\right]$$
$$q_{\vec{\tau}}(t)|_{(x,y)\in K_i} = w_3, \quad \forall u_{\vec{n}} > 0$$

Above, w_1 and w_3 are control variables, while w_2 is the outgoing characteristic variable to be extrapolated to the center of the cell $K_{i,n}$ from the interior along the direction normal to the edge $E_{i,n}$. For extrapolation we use a cubic spline representation of w_2 built in the vicinity of Γ_3. Similar expressions are used for the 'outlet' boundary Γ_4.

3.2 1D scheme

Assuming the Euler explicit time discretization, for a given finite volume $\tilde{K}_i$ the 1D model can be represented in the finite-dimensional form as follows

$$\tilde{U}_i'(t_{\tilde{m}}+\tilde{\tau}) = \tilde{U}_i'(t_{\tilde{m}}) - \tilde{\tau}\left(\frac{1}{|\tilde{K}_i|}\sum_{n=1}^{2}\tilde{F}_n(\tilde{U}_i') - \tilde{S}(\tilde{U}_i') - \Psi_i\right)_{t=t_{\tilde{m}}} \tag{9}$$

where $\tilde{m} = 0, ..., T/\tilde{\tau}$ is the time index, $\tilde{\tau}$ is the time step used for the 1D model integration, $\tilde{F}_n(\tilde{U}_i')$ are the fluxes of $\tilde{U}'$ via n^{th} edge of $\tilde{K}_i$, which can also be defined by the same steps as in the 2D case when using $\theta_1 = 0$, $\theta_2 = \pi$.

4 COUPLING CONDITIONS

4.1 2D → 1D information transfer

Flux term A first approach is to compute overflowing of the main channel as fluxes via its boundaries based on a current approximation of the 2D flow given by a 'zoom' solution. Thus, we define these fluxes as piece-wise constant functions G along the boundaries Γ_1 and Γ_2 as follows

$$G|_{\Gamma_1} := \{F_n(U_i')\}, \quad \forall (i,n): \ E_{i,n} \in \Gamma_1 \cap \Omega_2, \ K_i \in \Omega_1$$

$$G|_{\Gamma_2} := \{F_n(U_i')\}, \quad \forall (i,n): \ E_{i,n} \in \Gamma_2 \cap \Omega_2, \ K_i \in \Omega_1$$

Since the 1D state consists of the components (H', Q'), we need to retain only two first components of $G = (G_1, G_2, G_3)^T$, which we denote as $G_\perp = (G_1, G_2)^T$. Let us relate the 1D finite volume $\tilde{K}_i \in (x_1', x_2')$ and a segment of the main channel confined by the perpendiculars to the median curve at the points x_1' and x_2', and by the arcs they cut from the boundaries Γ_1, Γ_2, which we denote $\tilde{\Gamma}_{1,i}$ and $\tilde{\Gamma}_{2,i}$ (as we show in Fig.2). Then the overflowing in the 1D model can be compensated using the source term Ψ_i as follows

$$\Psi_i(t_m) = \frac{1}{\tilde{\tau}|\tilde{K}_i|}\int_{t_{\tilde{m}}}^{t_{\tilde{m}}+\tilde{\tau}}\left(\int_{\tilde{\Gamma}_{2,i}} G_\perp d\Gamma - \int_{\tilde{\Gamma}_{1,i}} G_\perp d\Gamma\right) dt \tag{10}$$

Flux term with defect correction A more general approach is based on the idea of a defect correction originated from the multi-grid method, see e.g. [5]. If A_f and A_c are spatial operators defined on a 'fine' and a 'coarse' grid correspondingly, U is a state variable and R is a fine-to-coarse projection (restriction) operator, then the 'defect correction' term used in the coarse grid problem approximation reads as follows

$$d = RA_f(U) - A_c(RU)$$

Let us define a piece-wise constant function $G(U')$ such that

$$G(U') = \left\{ \frac{1}{|K_i|} \sum_{j=1}^{4} F_j(U'_i) - S(U'_i) \right\}; \quad \forall i: \ K_i \in \Omega_1 \cap \Omega_2$$

This is the action of the finite-dimensional 2D SWE spatial operator on a state vector U', as in (7). Again, we need to retain only two first components $G_\perp = (G_1, G_2)^T$. Another function to be defined is the action of the finite-dimensional 1D SWE spatial operator on a state vector $\tilde{U}'$ (9) as follows

$$\tilde{G}(\tilde{U}') = \left\{ \frac{1}{|\tilde{K}_i|} \sum_{j=1}^{2} \tilde{F}_j(\tilde{U}'_i) - \tilde{S}(\tilde{U}'_i) \right\}; \quad \forall i: \ \tilde{K}_i \in \Omega_1 \cap \Omega_2$$

Now we introduce a projection (restriction) operator R that computes average values over $\tilde{K}_i$ and $\tilde{\tau}$

$$R_i(t_m)v = \frac{1}{\tilde{\tau}|\tilde{K}_i|} \int_{t_m}^{t_m+\tilde{\tau}} \int_{\tilde{K}_i} v \, d\Omega dt$$

Eventually, we compute the source term for the 1D model as follows

$$\Psi_i(t_m) = d_i := R_i(t_m)\, G_\perp(U') - \tilde{G}(R_i(t_m)\, U') \tag{11}$$

Let us note that for matching grids and without friction, the function Ψ_i obtained by (10) and (11) are equivalent.
Obviously, the defect correction term as specified in (11) is a generalization of the classical multi-grid defect correction, since it takes into account the dimensional heterogeneity.

4.2 1D → 2D information transfer

For coupling the 1D and 'zoom' models at the lateral boundaries we use a characteristic approach. Actually we demand that the total quantity of the incoming characteristic variables across the boundary must be preserved. This condition can be written as follows

$$\int_{\Gamma_3} w_1(x', y', t)\, d\Gamma = W_1(x', t)|_{x' \in \Gamma_3}, \ \int_{\Gamma_4} w_2(x', y', t)\, d\Gamma = W_2(x', t)|_{x' \in \Gamma_4} \tag{12}$$

where w_1, w_2 are defined in (2)-(3) and W_1, W_2 in (4)-(5) for arbitrary x'.
In the finite-dimensional implementation, the right-hand sides in (12) are computed from

known coarse grid values $W(x'_i, t_m),\ x'_i \in \tilde{K}_i$ using the cubic spline interpolation operator I, that can be written in the form

$$W_1(x', t)|_{x' \in \Gamma_3} = IW_1(x'_i, t_m), \quad W_2(x', t)|_{x' \in \Gamma_4} = IW_2(x'_i, t_m) \tag{13}$$

Let us note that no more information can be extracted from the 1D model. The distribution of w_1, w_2 on y' remains unknown as well as the tangent velocity w_3 in (3), because there exists no related quantity in the 1D formulation. This is a main problem of coupling dimensionally heterogeneous models.

5 THE JOINT ASSIMILATION-COUPLING ALGORITHM (JAC)

We present our method that allows to assimilate local data measured within 'zoom' areas into the 1D-net model. It is based on an optimal control process, which consists to minimize a cost function including the coupling boundary conditions terms (characteristics) and a term measuring the discrepancy between the full model response and observations. Hence, we do couple the 1D and 2D models (in a weak sense), while we identify inflow BC, both using the available data. The 2D model plays the role of a finer zoom model superposed to the global 1D network model.

To achieve this, we introduce the following objective functional:

$$J = \gamma J^* + J_1 + J_2 \tag{14}$$

This functional comprises a regular data assimilation term (weighted by γ)

$$J^* = \sum_i \int_0^T (U_i - \hat{U}_i)^2 \, \beta_i \, dt \tag{15}$$

where β is an array of dimension $(i_{max} \times 3)$, such that $\beta_{i,l} = 1$ indicates the finite volume number K_i, where the $l-$ component of the state vector is measured. Also, the functional comprises coupling conditions (12) in a 'weak' form as follows

$$J_1 = \int_0^T (\int_{\Gamma_3} w_1(x', y', t) d\Gamma - I\, W_1(x'_i, t_m))^2 dt \tag{16}$$

$$J_2 = \int_0^T (\int_{\Gamma_4} w_2(x', y', t) d\Gamma - I\, W_2(x'_i, t_m))^2 dt \tag{17}$$

This arrangement leads us to a 'one-way relaxed' model formulation, which can be defined by the following steps, see Fig. 3:

a) given the initial condition and a current estimation of boundary conditions $w_1(t)|_{\Gamma_3}$, $w_2(t)|_{\Gamma_4}$, $w_3(t)|_{\Gamma_{3,4}}$, solve the 2D 'zoom' problem for $t \in (0, T)$, (keeping the 2D flow field values at the sensor locations);

b) compute source terms to the 1D model $\Psi_i(t_m)$ using (11);

c) given the initial condition, current estimation of boundary conditions $W_1(0,t)$, $W_2(L',t)$ and $\Psi_i(t_m)$, solve the 1D problem for $t \in (0,T)$;

d) compute $W_1(x'_i,t_m)$ and $W_2(x'_i,t_m)$, $m=0,...,T/\tilde{\tau}$ using (13);

e) compute the value of the generalized objective functional (14) using definitions (15)-(17).

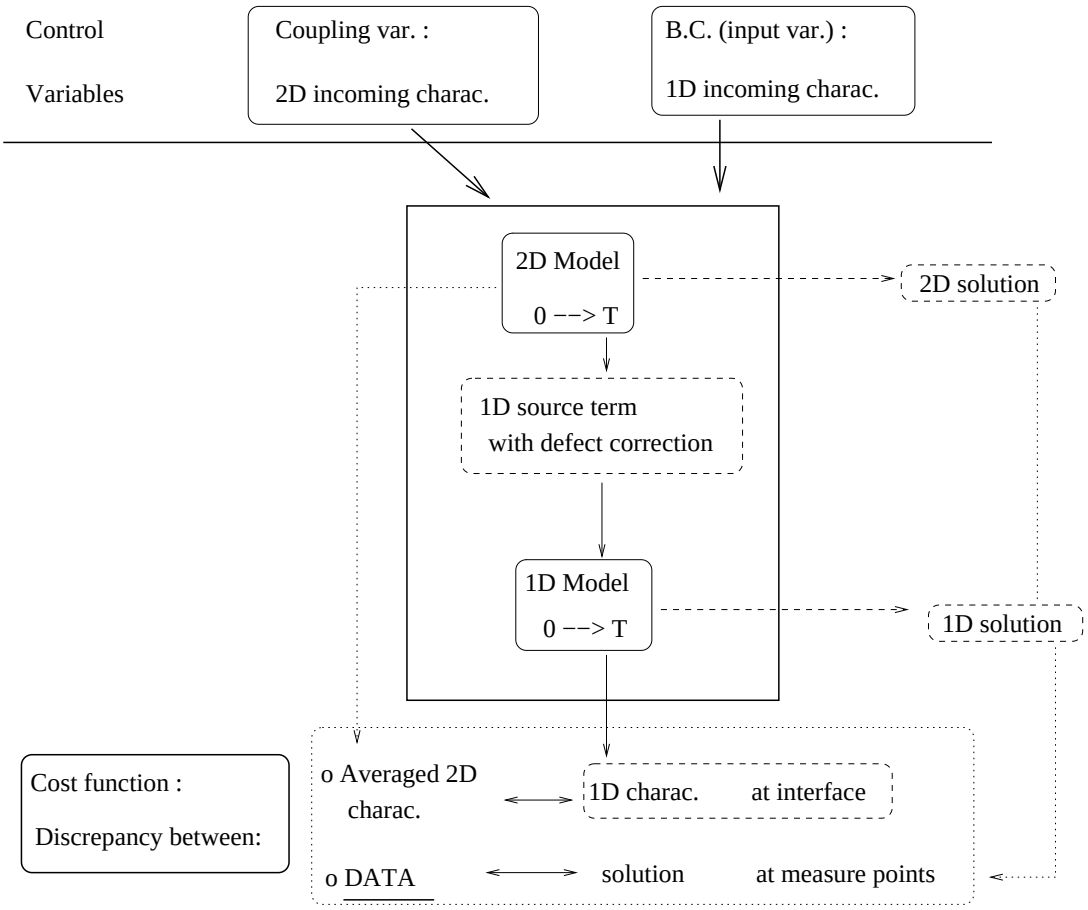

Figure 3: The Joint Assimilation - Coupling algorithm

Eventually we formulate the optimal control problem as follows:

$$\text{Find } \inf_{\vec{W}} J(\vec{W}) \tag{18}$$

with $\vec{W} = \left[W_1(0,t), W_2(L',t), w_1(t)|_{\Gamma_3}, w_2(t)|_{\Gamma_4}, w_3(t)|_{\Gamma_{3,4}}\right]^T$, and assuming the model constraints are defined by steps a)-c).

We refer to this control approach as to the Joint Assimilation Coupling (JAC) method. We must point out that no additional assumptions have been involved into the JAC model formulation: the lack of information is naturally compensated from the measured data.

Adjoint code and minimizer In order to implement the JAC method, we need the gradient of (14) with respect to the vector-function of controls $\vec{W}$. To this end we have differentiated the code implementing the 'one-way relaxed model' (as defined by items **a)-d)**) plus the objective functional. This task has been completed by means of the Automatic Differentiation tool TAPENADE developed at INRIA, TROPICS [10]. The resulting adjoint code has been optimized and verified using classical tests. For optimization we use the quasi-Newton LBFGS algorithm with the Wolf linear search.

6 NUMERICAL RESULTS

For all numerical tests, we have used a simplified problem layout as shown in Fig.4(left). The boundary at $y = 0$ (Γ_1) is the no-flow boundary, i.e. a wall. For simplicity, lateral

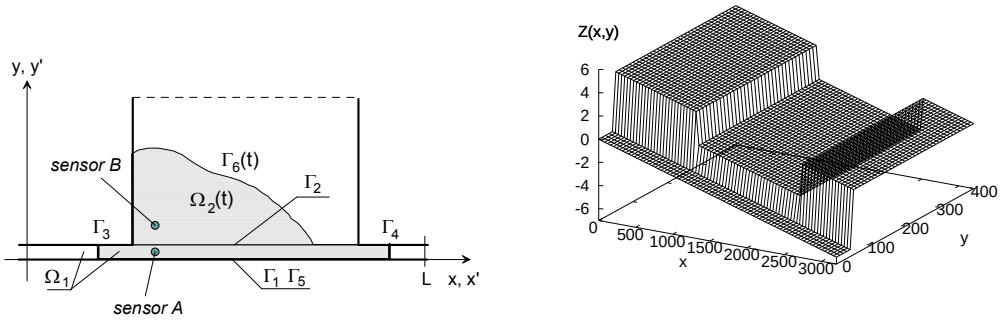

Figure 4: Simplified problem layout and bathymetry used in numerical tests

boundaries of the 'zoom' area Γ_3, Γ_4 are chosen beyond the area where the overflowing may happen. Despite a simplification this idealized scheme allows verifying the basic ideas of the proposed approach. More complicated situations require the non-uniform mesh to be used, that we have tried to avoid. The bathymetry with a uniform bed slope in the x-direction as shown in Fig.4(right) is used. The main channel width is 40m. In simulations, the 1D model is solved using the 1D option of the same 2D solver.

6.1 The reference solution

To enable analysis of results, we compute a 'reference' flow pattern by solving the 2D problem in the entire spatial domain $\Omega_1 \cup \Omega_2$. As the initial condition we use a steady-state flow confined by the main channel. This flow is supported by a constant value of the inlet boundary control $W_1(0,t)$ (at the outlet we always keep an 'open boundary', assuming $w_2(L',t)=0$). Then we add a time-dependent component, which creates a wave propagating downstream. When the wave reaches the 'low bank' it starts overflowing and produces a wetting front travelling over the previously dry area. This process is illustrated in Fig.5, where the surface elevation of the flow in Ω_2 for different time instants is presented. The boundary condition that generates the reference solution is as follows

$$W_1(0,t) = [0.5 + 1.2\left(1 + sin\left(\frac{3\pi}{2} + \frac{\pi t}{480}\right)\right)]\ 10^4\ m^2/s$$

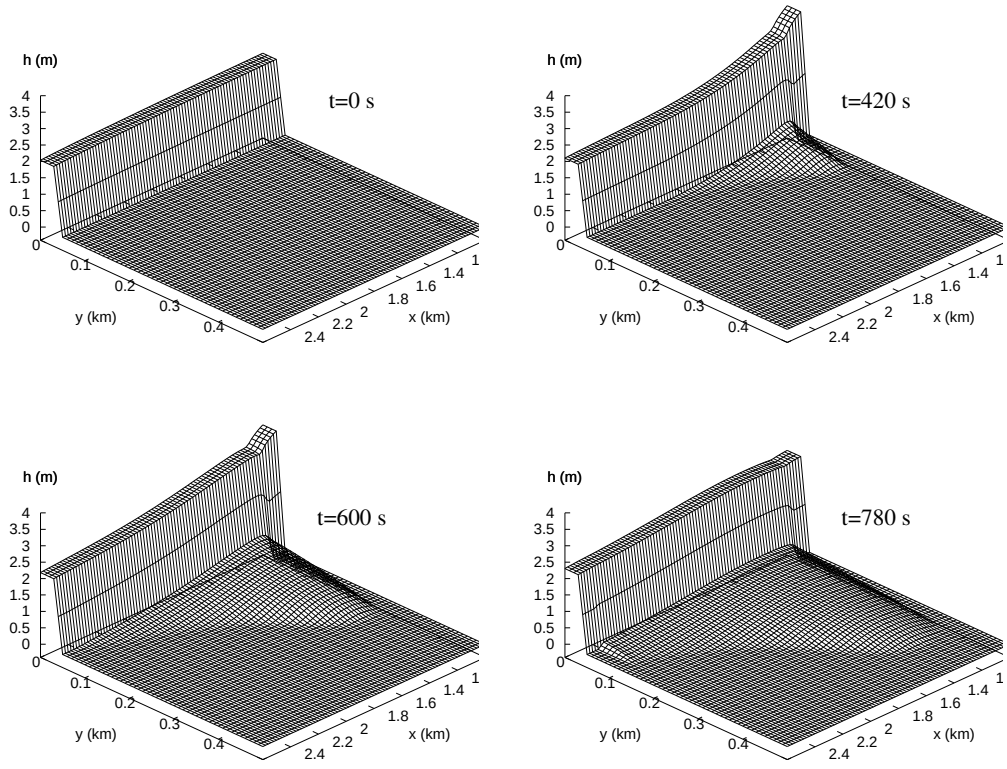

Figure 5: Reference flow (surface elevation h) for different times

We speak about 'consistent discretization' when the 1D model solution is obtained with the same space mesh $h'_x = h_x$ and time step $\tilde{\tau} = \tau$ as 2D problems, and about

'inconsistent discretization' otherwise.
The unknowns of the 2D model are the incoming characteristic variables $w_1(t)|_{\Gamma_3}$ and $w_2(t)|_{\Gamma_4}$, while for the 1D model we seek to identify the upstream incoming characteristic variable $W_1(0,t)$, assuming the open boundary at $x = L'$, see Fig. 3.
Data is collected in two points located within the 'zoom' area (see Fig.4,left). The exact location of the sensors is as follows: $x_1 = 290\,m, y_1 = 20\,m$ for sensor A, $x_1 = 290\,m, y_2 = 140\,m$ for sensor B. Measurements to be used in the identical twin experiment are generated by the 2D reference solution.

6.2 Results with a consistent discretization

In the following assimilation examples presented in Fig.6, Fig.7 we use a consistent discretization. Here to the left, we can see the reference BC (in dashed line) and the retrieved value after k iterations of the JAC algorithm (in sharp solid lines). A line that corresponds to $k = 0$ is the initial guess. To the right, one can see the convergence history for J and for its components J^*, J_1, J_2. These examples show that the JAC method converges and allows retrieving the unknown BC of the 1D model, while data is assimilated into the 'zoom' model. When both q, p and h are measured (Fig.6) we need just 10 iterations to get quite a reasonable approximation of the reference value, about 20 iterations to get a very close one (apart from the 'blind' spot in the vicinity of $t = T$, where the BC cannot be obtained in principle).
When only h is measured, one needs more iterations to get a good quality approximation of $W_1(0,t)$, although any difference in the convergence rate cannot be seen.

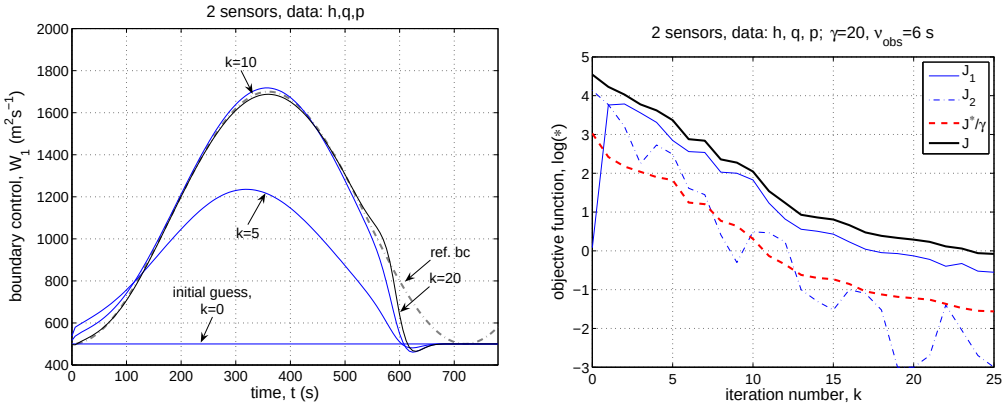

Figure 6: Consistent discretization. Assimilation of data (h, p, q) by the JAC algorithm: $W_1(t)$ after k iterations (left); Convergence history in log scale (right).

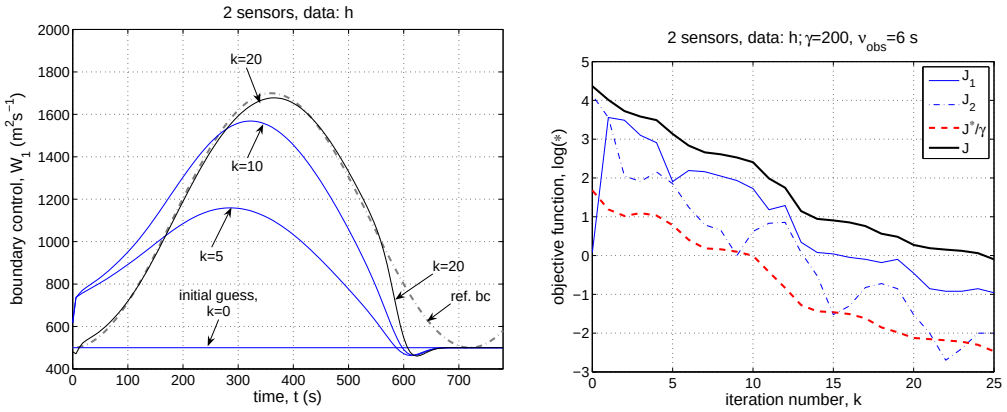

Figure 7: Consistent discretization. Assimilation of data (h) by the JAC algorithm: $W_1(t)$ after k iterations (left); Convergence history in log scale (right).

6.3 Results with an inconsistent discretization

In the next data assimilation example (Fig.8), we use an inconsistent discretization where $\tilde{\tau}/\tau = 10^2$, $\tilde{h}_x/h_x = 10^1$ and h-data only. As above, to the left we show the reference BC and the retrieved value after k iterations; to the right - the convergence history. One can see that the convergence rate is the same as in the previous example, but the retrieved value of $W_1(0,t)$ deviates from the reference value. This probably happens because the 1D model is solved used a very coarse discretization steps and the solution error accumulates beyond the 'zoom' area. There exists such an iteration number k_{opt} when we get the best approximation of the reference value ($k \approx 12$). As we proceed iterating, the estimation deviates from it approaching the value shown at $k = 20$. If the 1D problem boundary control is a purpose by itself, one should look for an appropriate stopping criteria. However, within Ω_2, the 'zoom' solution perfectly reproduces the reference solution; within $\Omega_1 \cap \Omega_2$, the 1D coupled solution perfectly reproduces the reference solution too (as good as the space discretization allows), but beyond this domain may deviate, see Fig.9.

In conclusion, one can say that the 'zoom' model may be regarded as an operator that maps measured physical quantities into the state space of the basic model.

6.4 Results with sensor B only

In the last numerical test, we consider a consistent discretization and we assimilate data into the zoom model only. These data are not represented in the basic model i.e. 1D model. We consider only the data collected by the 'dry field' sensor B, Fig.1(right), located at $y' = 100\,m$ from the overflowing boundary Γ_2). To set up an ultimate test

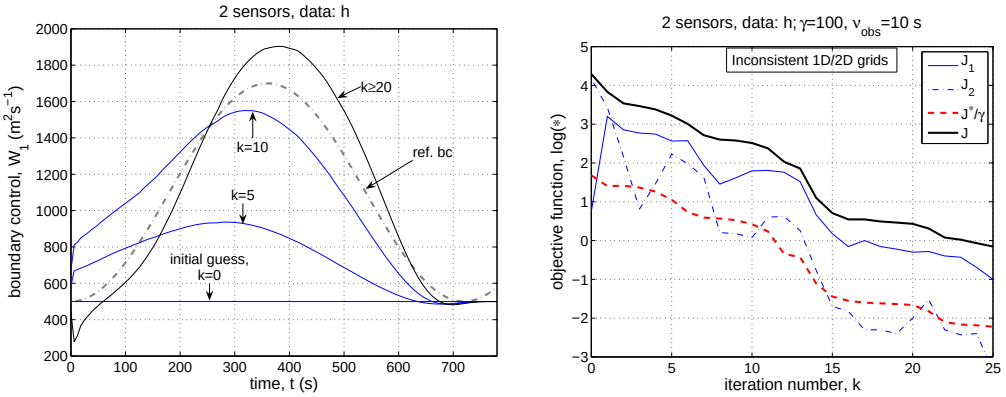

Figure 8: Inconsistent discretization. Assimilation of data (h) by the JAC algorithm: $W_1(t)$ after k iterations (left); the convergence history (right).

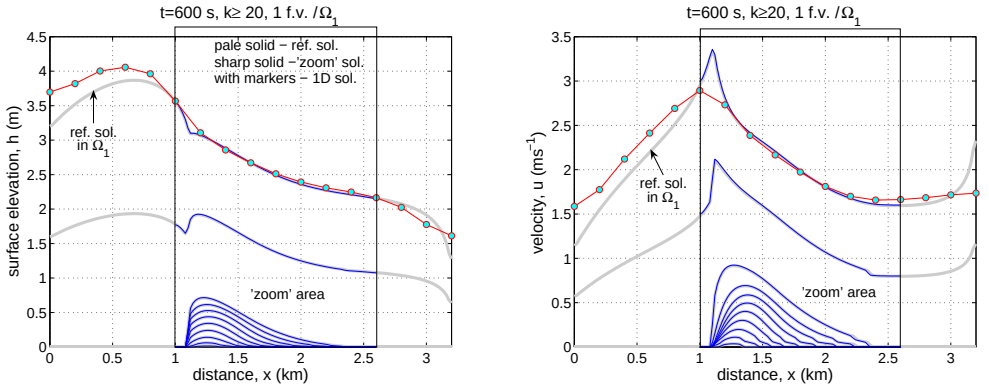

Figure 9: Solution after DA (corresponds to Fig.8). Elevation (left) and velocity (right).

case we use a special form of the reference BC as shown in Fig.10(left) by a dash-dotted line. One can see that up to $t \approx 300\,s$ the value of control does not exceed a flood trigger level. This is done to increase a period when sensor B remains 'dry'. The readings of the sensor are shown in Fig.10(left) by solid lines. We note that up to $t \approx 600\,s$ all measurements remain zero. The problem solution obtained by the JAC algorithm is presented in Fig.10(right).

Here, by a dash-dotted line we show the reference BC and by solid lines - the retrieved value after k iterations. The only 'trick' in solving this DA problem is that one must start iterations from the initial guess that necessarily keeps the whole domain Ω_2 wet (solid line, $k = 0$). As a result we manage to identify quite satisfactory a part of the unknown boundary control between $t \approx 300 - 750\,s$, i.e. the part, which is actually responsible for causing a flood event. The part below the flood trigger level is not retrieved, neither,

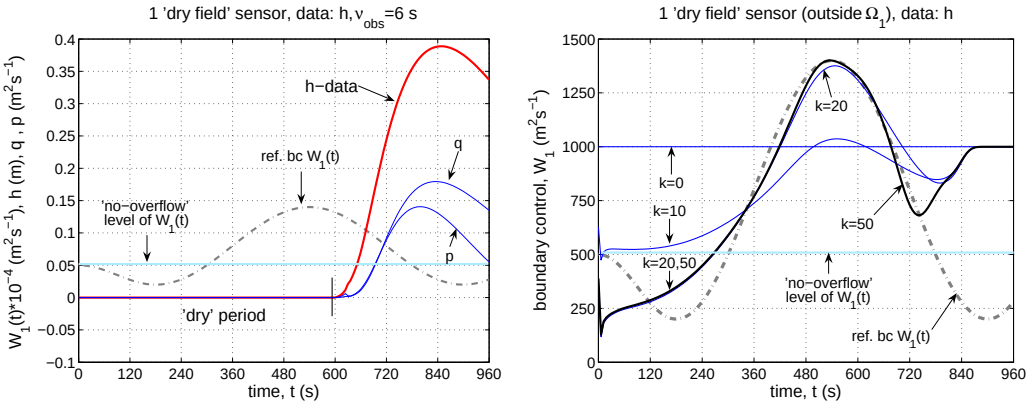

Figure 10: Reference BC and readings by the 'dry field' sensor B (left). Assimilation of data (h) by the JAC algorithm: $W_1(t)$ after k iterations (right).

of coarse, the solution in a certain vicinity of the terminal point $t = T$. It is worth mentioning that the solution has been identified for times far preceding to the beginning time of the 'wet' period for the sensor B ($t > 600\,s$). We should stress that this result could not be obtained in the framework of the 1D model in principle.

7 Conclusion

Global numerical models cannot always consider natural phenomena in full complexity and everywhere because of computational difficulties. Actually, this is not always necessary, but in some parts of the problem domain the effects which are not represented by the global model become important and must be taken into account. Hence, 'richer' local models may become interesting. Also, in the DA context, richer local models may allow to assimilate measured physical quantities which are not the variables of the basic global model. In some cases the correspondence between them could be easily established, in some cases could not. If the extra state variables of a richer local model match with some of measured quantities, it can be viewed as a mapping operator.

We present here a weak and superposed coupling method. That is, the richer local model is laid over the global model in some area, which can be chosen either from physical considerations or by a-posteriori estimates. The global model provides a basis for estimating the local model open BCs, while the richer local model produces 'defect correction' source terms that allows adjusting global model solution into the local 'zoom' area. Such an approach keeps the integrity of the global model. Also, for the DA context, 'zoom' richer models may be considered as a part of the sensor supply, making the instrumental devices compatible with the basic global model.

This is the idea we developed here, as applied to river hydraulics modelling. As global model, we have the 1D shallow water model with storage areas. Over the storage areas,

we superpose a local zoom 2D shallow-water model. Then, we builted, what we called, the Joint Assimilation Coupling (JAC) algorithm, which treats simultaneously the assimilation and weak coupling problems through minimizing an extended objective functional. It is based on the optimal control method. A lack of information is compensated from measured data, hence no extra a-priory information is needed.
For this application, we have developed the information exchange principles (based on incoming characteristics) and tested them numerically for a simplified problem layout. The numerical experiments show that the global model gets obvious benefits from using a zoom richer local model, and demonstrate the efficiency of the coupling method, which converges in few iterations. In the last numerical test case presented, elevation data located outside the 1D main channel have been successfully assimilated, and allowed to retrieve the most important part of the unknown inflow BC of the 1D model that caused the 'flooding'. This information could not be considered using the 1D-net global model only.

REFERENCES

[1] L. Formaggia, J.F. Gerbeau, F. Nobile and A. Quarteroni, *On the coupling of 3D and 1D Navier-Stokes equations for flow problems in compliant vessels*, Comput. Methods Appl. Mech. Engrg., 191(2001) 561-582

[2] E. Miglio, S. Perotto and F. Saleri, *Model coupling techniques for free-surface flow problems*, Part I, Proceedings of the Fourth World Congress of Nonlinear Analysis WCNA-2004, Orlando, Florida, USA (2004)

[3] M. Bjorhus, *On domain decomposition, subdomain iteration and waveform relaxation*, PhD Thesis, University of Trondheim, Norway (1995)

[4] P. Gervasio, J.L. Lions and A. Quarteroni, *Heterogeneous coupling by virtual control methods*, Numer. Math., 90 (2001) 241-264

[5] A. Brandt, *Multi-level adaptive solutions to boundary-value problems*, Math. Comp., 31 (1977) 333-390

[6] B. Engquist and A. Majda, *Absorbing boundary conditions for the numerical simulation of waves*, Math. Comp., 31 (1977) 629-651

[7] E. Blayo and L. Debreu, *Revisiting open boundary conditions from the point of view of characteristics variables*, Ocean modelling, 9 (2005) 231-252.

[8] E.F. Toro, *Shock-capturing methods for free-surface shallow flows*. J. Wiley and Sons (2001)

[9] R.J. Le Veque, *Balancing source terms and flux gradients in high-resolution Godunov methods: the quasi-steady wave propagation algorithm*, J. Comp. Physics, 146 (1998) 346-365

[10] A. Hascoet and V. Pascual, TAPENADE 2.1 user's guide, Technical Report RT-300, INRIA, 2004